Purification and characterization of checkpoint blockade enhancing molecules from Coprobacillus cateniformis.

Purification and characterization of checkpoint blockade enhancing molecules from *Coprobacillus cateniformis*.

Jason Daugherty

A Thesis in the Field of Biotechnology

for the Degree of Master of Liberal Arts in Extension Studies

Harvard University

May 2024

Abstract

Checkpoint blockade treatment enhancement is one of the frontline areas of study in cancer treatment, however it comes with two large drawbacks, the limited number of cancer lines in which efficacy is shown and the difficulty in tolerating the treatment. An increase in the efficacy of checkpoint blockade treatment has been shown to correlate to the presence of individual members of the human gut microbiota and the microbial contributions to immune training and regulation within the host. *Coprobacillus cateniformis* has been shown to enhance anti-PD-L1 and anti-PD-L2 treatments in a mouse tumor model, even when cotreated as a dead bacteria indicating the presence of an immunomodulatory molecule on the surface of the bacteria. I compared three chemical extraction techniques to determine the most efficient and effective method for molecular isolation. After isolation, I used low pressure size exclusion chromatography paired with a second ion exchange chromatography method to remove superfluous bacterial extract products. Further characterization of the bacterial product was performed through chemical analysis via gas chromatography mass spectroscopy, enzymatic degradation, and NMR spectroscopy. The sum total of the chemical analysis led to the characterization of a small surface associated bacterial lipid that may be attached to a xylose polysaccharide that we have shown increases the efficacy of anti-PD-L1 and anti PD-L2 treatments in our mouse tumor models.

Table of Contents

List of Figures

Chapter I.

Introduction

Cancer treatment is an increasingly challenging treatment problem in the field of medicine. With approximately 1.9 million new cases predicted to be diagnosed and upwards of 600,000 deaths (American Cancer Society 2023) it is predicted to be one of the leading causes of death in the United States. Treatments for many forms of cancer can be difficult for patients to tolerate, ranging from chemotherapy cocktails with significant side effects and risks to major surgeries that have long lasting consequences. This has led to increased interest in treatments that leverage our innate immune systems regulatory functions in order to treat cancer diagnoses. It has been shown that targeted immunotherapeutic treatments can have similar positive effects for patients while having less severe side effects for patients. (Tan, Li, and Zhu 2020) In order to develop effective immunotherapeutic treatments for the multitude of cancer strains prevalent in the patient population a thorough understanding of the biochemical tactics tumor cells use to evade the immune system is necessary.

Immunosuppression in tumor cells

The human immune system works to identify both internal and external pathogens and dispose of them in order to maintain homeostasis. For a tumor to thrive and reach the point of risk to a patient it must employ strategies in order to evade the natural immune response that would eliminate it. Cancer cells have been shown to accomplish this through the implementation of multiple strategies.

The first being through general immune suppression in the tumor microenvironment. Some tumor strains can control the prevalence of certain metabolites in the tumor microenvironment that lead to an increase in immunosuppressive T regulatory cells (Jacobs et al 2012). Proposed methods for attempting to counteract this metabolic evasion system involve the targeting of specific metabolic pathways within the cancer cells with metabolite analogues that would hopefully restore host immune activity. These strategies are not yet well understood, and the clinical efficacy is still unproven. (Kyouidhi, Ayed, and Elgaaied 2018)

A second strategy seen in some tumor cell lines, especially many melanomas, is to interfere with the pathways that lead to effective antigen presentation in T cells. This was first seen in tumor mediated downregulation of the TAP-1 gene in some cell lines leading to deficient MHC class I antigen presentation (Seliger, Maeurer, & Ferrone 1997). Without this presentation the cytotoxic T lymphocytes are unable to recognize the tumor strains as targets.

Another strategy employed is the production, either directly or through non-tumor cells in the tumor microenvironment, or immunosuppressive cytokines. This appears to be primarily mediated through transforming growth factor beta (TGF-β) (Pasche 2001) as well as many other interleukin, interferon, and stimulatory factors. All of which lead to a combination of immune suppression and growth stimulation that overwhelm the normal immune response (Vinay et al 2015).

The final strategy, and the focus of this research, is on the ability of certain cancers to express cell surface antigens that allow them to counteract the natural immune response mounted by the host T cells. (Ribas & Wolchok 2018) This can often be

expressed through interference in pathways that activate CD8 positive cytotoxic T cells and CD4 positive helper T cells as well as the release of cytokines that increase the activity of regulatory T cells. This combination has the effect of significantly decreasing tumor killing activity. The immunosuppression is achieved through the inactivation of CD8 positive cytotoxic T cells, which otherwise would trigger cell death in tumor cells, and the inactivation of CD4 positive helper T cells, which normally act to stimulate killer T cells and other classes of immune cells that would target tumor cells. This is often coupled with the upregulation of regulatory T cells in the tumor environment. These regulatory T cells act to promote tumor growth by inhibiting the cytotoxic immune response in tumor environments (Zamarron & Chen 2011). Evidence seems to indicate that tumor cells manipulate the T cell populations through maintaining a chronic inflammatory environment (Coussens & Werb 2002) and through the secretion of cytokines that help to recruit regulatory T cells to the tumor environment and the conversion of CD4 positive T cells into regulatory T cells (Zou 2006).

In addition to influencing the populations of T cells in the tumor environment some tumors also act to manipulate cell surface signaling molecules. These tumor cells induce an environment that creates dysfunctional antigen-presenting cells leading to the induction of regulatory T cells. These regulatory T cells then express cytotoxic T-lymphocyte-associated protein 4 (CTLA-4) initiating a signal cascade that leads to the inactivation or death of cytotoxic T cells (Zou 2006). In addition to these regulatory T cell-mediated pathways, some tumor cell lines manage T cell populations through expression of surface binding proteins. Tumor cells have been identified that have increased expression of programmed cell death ligand 1 (PD-L1) and programmed cell

death ligand 2 (PD-L2). (Juneja et al 2017) These ligands act as a signal to T cells in the tumor environment that lead to an inhibition of T cell mediated immune responses. This is accomplished through decreased activation and proliferation of cytotoxic T cells as well as decreased cytokine secretion (Han, Liu, & Li 2020).

Checkpoint inhibitor treatments and their challenges

One of the first successful checkpoint inhibitor treatments was the discovery that interleukin-2 (IL-2) can be used to improve the outcomes of patients with melanoma (Marabondo and Kaufman 2017). This use of cytokines to improve cancer treatment inspired the search for other targets for molecular intervention in tumor mediated immunosuppression. The next advance in checkpoint inhibitor treatment originated in the discovery of the T cell regulatory effects of the cytotoxic T-lymphocyte-associated protein 4 (CTLA-4) and the corresponding effects on tumor growth (Leach et al 1996). Treatment with anti-CTLA-4 antibodies proved to create a robust and durable anti-tumor response in some patients but the treatment was plagued with issues of cytokine toxicity. This along with the realization that only a small population of tumors were susceptible to the treatment encouraged studies to identify other targets for checkpoint inhibition treatments (Snyder et al 2014 &Van Allen et al 2015).

The blockade of the PD-1 pathway was achieved through the development of antibodies that targeted PD-L1and PD-L2. Each of these ligands is sufficient to activate the PD-1 pathway on cytotoxic T cells and leads to them entering a chronic state of activation through repeated stimulation. This causes a dysregulated state referred to as T cell exhaustion and disables the cytotoxic T cells from effectively triggering cancer cell

death. The PD-1 pathway also appears to help with the overall modulation of T cell metabolism and exhaustion of the T cell system has larger impacts on the overall immune response (Lefleur et al 2002). While a robust and effective treatment for patients, it is estimated that only approximately 40% of cancers have immunotherapies with known effect and the efficacy rates in patients can be as low as 13% of all patients (Haslam & Prasad 2019; Zhao et al 2020) and with many patients exhibiting the same cytokine toxicity issues that were observed with other antibody-based therapies. (Ribas & Wolchok 2018)

Microbial enhancement of checkpoint inhibition treatment

The current best practice for improving the outcomes of checkpoint inhibitor immunotherapy is to screen for tumor strains that have known susceptibility to treatment and, where possible, administer a combination of non-redundant blockade treatments to maximize efficacy (Ribas & Wolchok 2018). It has long been known that the commensal bacteria present in the human gut microbiota influence the immune system and can contribute to improved health outcomes (Chung et al 2012). Through the comparison of specific pathogen free (SPF) and germ-free mice with established tumors that were susceptible to anti-CTLA-4 antibody treatment Vetizou et al (2015) showed that gut microbiota had a controlling influence on the efficacy of the treatment. They also observed that there were species dependent population differences that influenced the efficacy of the blockade treatment. Similarly, Sivan et al (2015) showed that the efficacy of an anti-PD-1 antibody treatment could be improved through the oral gavage of *Bifidobacterium*. This advance was not only important because it showed that the microbial enhancement of checkpoint inhibitor treatment was not isolated to a single

pathway but showed that the increase in efficacy could be coming from individual members of the microbiota instead of as the outcome of a holistic population effect.

Further work has shown that the composition of a patient's gut microbiota directly contributes to the efficacy of immune checkpoint treatments (Tanoue et al 2019) and have seen enhanced efficacy of the anti-PD-L1 checkpoint treatment specifically in patients with melanoma (Baruch et al 2021; Davar et al 2021). Further, Matson et al (2018) has shown that the composition of the gut microbiota can be used to effectively predict the efficacy of an anti-PD-1 checkpoint inhibitor treatment in patients with metastatic melanoma. These enhancing effects have been shown to be replicable in a mouse tumor model through colonizing germ-free mice with patient stool samples and observing the growth of cancer cell lines through an anti-PD-L1 dosage scheme (Gopalakrishnan et al 2018).

Griffin et al (2021) continued to show that the microbial enhancement of checkpoint blockade treatment could be isolated to a single bacterial metabolite and signaling pathway. They were able to show that *Enterococcus* bacteria with a specific peptidoglycan structure were able to increase tumor killing in anti-PD-L1 mouse models. They identified that this was done through the nucleotide binding oligomerization domain containing 2 (NOD2) signaling pathway leading to higher levels of T lymphocytes and higher expression of checkpoint related receptor signaling and increased markers of cytotoxic T cell activity. Through work in our lab, Park et al (2023) has shown that *C. cateniformis* alongside anti-PD-L1 checkpoint treatments enhances tumor killing in the mouse tumor model through its effect on the PD-L2-RGMb pathway.

Isolation of bacterial effector molecules

The immunomodulatory effects of the gut microbiome are evident in the enhancement of checkpoint blockade treatments and Griffin et al (2021) have shown that this enhancement can in some cases be isolated to a single class of bacterial metabolite or byproduct. Similarly, our lab has shown that specific bacterial byproducts, such as bacterial lipopolysaccharide (Erturk-Hasdemir et al 2019), can educate and enhance immune response in significant ways. Through identifying and characterizing the effector molecules produced by *C cateniformis* it may be possible to further understand the specific signaling pathways that are acted upon to induce the checkpoint enhancement and to better understand what other mechanisms can be exploited in order to expand the treatment efficacy to other cancer strains.

Park et al (2023) showed that gavaging mice with dead *C. cateniformis*, as an obligate anaerobe any handling outside of an anaerobic environment leads to complete bacterial inactivity, alongside the administration of anti-PD-L1 antibodies was sufficient to enhance tumor killing. This strongly indicates that the effector molecules were surface associated molecules. This was confirmed through in vitro testing of a rough surface extract obtained using a mutanolysin based processing method adapted from Deng et al (2000).

Isolation of an unknown bacterial model is a challenging task that can be approached using many techniques. Deng et al (2000) describes two methods that generated immunomodulatory material. The first being a mutanolysin based digestion of the bacterial cell wall through cleavage of the muramyl-glucosamine linkages in the peptidoglycan. In the same paper a base hydrolysis extraction is described to extract

polysaccharide from GBS type III. This extraction presents a simple and high yield extraction for surface polysaccharides that may be responsible for immunological activity. A final extraction technique that we have seen success with in *Bacteroides fragilis* is a hot phenol extraction that is described in Erturk-Hasdemir et al (2019). This technique is quite effective at purifying capsular lipopolysaccharides and lipooligosaccharides, both categories of molecules that have shown highly immunogenic activity.

Purification techniques

The first step in the purification of bacterial extracts is often accomplished through the application of liquid chromatographic separation techniques. This is accomplished through loading rough bacterial extracts that are suspended in the appropriate chemical buffers into a column that has been packed with a resin that has a physical property that will allow for differential retention of material. The common resins that are used in biological sample preparation provide for the separation of bacterial products based on their molecular size, ionic affinity, or hydrophobic interactions. (Wu 2004)

Size exclusion chromatography

Size exclusion resins are formulated to create a matrix that allows the column to catch a range of molecular weights. These size exclusion resins are usually measured for both globular proteins and for dextrans, standardized polysaccharides made from 1:6 linked glucose molecules. When samples are loaded onto a size exclusion resin any molecules present in the sample that are larger than the largest pores cannot enter the

matrix and elute in the void volume. All other molecules will travel through the matrix based on their molecular size and will elute from largest to smallest with molecules smaller than the pores eluting slightly before a single column volume.

Size exclusion chromatography has both the benefit and drawback of being agnostic to the chemical compositions of any biological extract. It can be affected by hydrophobic, and charge based chemical moieties, these chemical phenomenon can cause the molecules to group together in micelles and other larger conglomerates. This can be overcome by varying the composition of the running buffers that are used with the size exclusion column, either through the addition of a detergent or surfactant if lipid micelle formation is noticed or through varying the buffer compounds, pH, and strength if there are electrochemical moieties that lead to compound aggregation. (Cytiva 2020)

Ionic affinity chromatography

Ionic affinity separates molecules based on their total surface charge of a molecule. The resins that are used in ionic affinity chromatography are composed of beads with chemical modifications that give them an overall ionic affinity. The chemical composition of the resin will have an overall anionic (negative) or cationic (positive) affinity and will retain molecules that have an opposite total surface charge.

Unlike size exclusion where compounds will elute based on the volume of running buffer that the column is subjected to, ionic affinity elutes compounds based on the ionic strength of the running buffer. The ionic attraction that the resin relies on can be counteracted through increasing the ionic strength of the running buffer, allowing samples to be fractionated according to a specific and repeatable ionic strength. To take advantage of these electrochemical interactions biological extracts are often loaded in

low ionic strength buffers or low concentration salt solutions and using a dual pump gradient eluted along a gradient of increasing ionic strength. If the biological sample involves a complex combination of molecules, it can also be beneficial to use a stepwise gradient in order to create clear fractionation according to the ionic strength of the eluent. (Cytiva 2021)

Hydrophobic interaction chromatography

Hydrophobic Interaction separates molecules based on the hydrophobicity of the molecule's chemical moieties. These columns are packed with resin that has carboxyl chains of known length embedded in the surface of the resin. The length of these chains, usually ranging from eight to eighteen carbons long, help to moderate the strength of interaction that a sample has with the column material, with longer chains having a stronger hydrophobic binding potential. The higher binding potential allows for the retention of biological extracts with weaker hydrophobic chemical moieties but comes with the complication of needing to use stronger solvents to elute the compounds from the column.

Like ion exchange chromatography bacterial extract material is usually loaded onto the column in neutrally buffered salt solution and then fractions are eluted off the column using a solvent mixture of increasingly hydrophobic nature. This is accomplished either using a solute gradient on a high-pressure liquid chromatography system or if conducted using a solid phase cartridge by the application of increasingly hydrophobic solvents, usually solvents like acetonitrile, isopropyl alcohol, and hexane. (Agilent 2016)

Characterization of biological molecules

Most biological extracts contain a diverse mixture of polysaccharides, lipids, proteins, and other metabolites. While previously discussed chromatographic techniques can provide insight on the characteristics of the molecules being studied some further specific analysis is sometimes required. Nuclear magnetic resonance (NMR) spectroscopy is a technique where biological samples are exposed to strong magnetic fields that cause the nuclear spin state of atoms within the molecule to take on a normalized spin state. The sample is then exposed to a pulse of radio frequencies that cause the normalized state to become excited and the vibrational frequencies of each atom are recorded as they relax back to the normalized state. These frequencies correspond to the chemical environment of each atom, and have very reliable and predictable values based on the chemical bonds that the atoms are a part of. The most frequently used NMR analysis involves observing the chemical environment around hydrogen atoms in a sample. These can provide strong indicators for the presence of carbohydrates, lipids, and nitrogen containing compounds based on their signal strength (Marion 2013).

Another technique common in biological sample determination is the use of a mass spectrometer in tandem with either gas or liquid chromatography. Mass spectrometers measure the mass to charge (m/z) ratio of ions that are present in your sample, this coupled with the use of databases of biological samples can sometimes help to identify common biological structures in your sample. The most relevant techniques to this work are gas chromatography mass spectroscopy (GC-MS), in which a volatile sample is vaporized at high temperature causing the ionization of any molecules in a

sample and is then separated on a silica column using an inert carrier gas before the ion detector reads the m/z of ions as they elute off the column or liquid chromatography mass spectroscopy (LC-MS) in which a previously discussed form of liquid chromatography is paired with an ion source and mass spectrometer. The ion source most used in biological assays is an electron spray ionizer. This method applies a strong charge to the sample inlet stream as it is pushed through a capillary causing the stream to be converted into a fine mist. A heated neutral gas, normally nitrogen, is sprayed along the capillary that causes the droplets to evaporate leaving any sample carried in them with the charge that the capillary applied to the stream. These ionized molecules are then drawn into the mass spectrometer and are analyzed (Finehout & Lee 2003).

Chapter II

Methods and Materials

The study set out to extract and evaluate the specific bacterial antigens that were present in *Coprobacillus cateniformis*. I developed the following techniques for bacterial growth, molecular purification, and chemical analysis from previously established techniques in the Kasper lab.

Growth and preparation of *C. cateniformis*

Each batch of *C. cateniformis* was prepared from an aliquoted stock solution that is stored at -80 degrees in order to maintain sample integrity. The growth process was started by taking a frozen aliquot and plating onto a brucella blood agar plate and incubating overnight in an anaerobic environment. This plate was used to create a starter culture by inoculating 50 mL of autoclave sterilized Reinforced Clostridia medium (RCM) with growth from the plate and allowing to culture overnight. The starter media was used to inoculate bottles of autoclave sterilized RCM that had been allowed to equilibrate in the anaerobic chamber at a rate of 3.33 mL of inoculant per liter of sterilized RCM. Optimal culture density was achieved by allowing the inoculated bottles to culture between 48-72 hours.

After culturing *C. cateniformis* in the anaerobic chamber samples from each bottle were taken and prepared for 16s sequencing in order to determine if there was any contamination of the inoculated bottles. Bacterial growths were stored at 4 C after having

sodium azide added at sufficient concentration to prevent further bacterial growth. Once 16s sequencing confirmed sample integrity the growth medium was centrifuged for 30 minutes at 8,000 RCF and 4 C. Bacterial pellets were then immediately processed according to the chosen extraction method.

Extraction of bacterial molecules from whole bacteria

Unless otherwise stated all water that was used in the extraction and purification of bacterial fractions was type I water certified to be free of any immunologically active contaminants.

Base hydrolysis

Bacterial pellets were suspended in 1N Sodium hydroxide at a four to one ratio volumetrically. The suspension was incubated at 37 C for 36 hours on a stir plate. After incubation the suspension was neutralized using 11.6 M Hydrochloric acid and was centrifuged for 30 minutes at 8,000 RCF at 4 C, collecting the supernatant and discarding the pellet.

The supernatant was then dialyzed using a three kilodalton (kDa) membrane in order to remove excess salts and to concentrate the bacterial extract. After dialysis the sample was frozen and lyophilized to prepare it for chromatographic fractionation.

Hot phenol extraction

The bacterial pellets were suspended in water and brought up to 68 C in a water bath located in a fume hood. Sterilized glass beads were added to the solution and warmed phenol was added to a final concentration of 37.5% phenol. The solution was

agitated by a Teflon paddle for 30 minutes while being held at 68 C. After this the extract had a sterilized magnetic stir bar added and was incubated at 4 C overnight on a stir plate. The phenol water solution was centrifuged in phenol resistant bottles for 30 minutes at 10,000 RCF and 4 C. The aqueous phase was reserved, and the phenolic phase and pellet were discarded.

The aqueous phase was added to a separatory funnel and an equal amount of diethyl ether was added and thoroughly mixed until a homogenous mixture was achieved. This mixture was allowed to sit overnight to allow for phase separation. After the phases separated the aqueous portion was kept and the diethyl ether portion along with any interface material was discarded. The diethyl ether wash was repeated and allowed to separate, approximately 1 hour on second wash, and again the aqueous phase was reserved, and the diethyl ether and any interface was discarded. Any trace amounts of diethyl ether were removed by processing the sample on a rotary evaporator at 40 C and 50 mTorr until evaporation ceased and the smell of diethyl ether was removed from the extract. The aqueous phase was then dialyzed using a three kDa membrane to remove excess salts and concentrate the sample before being frozen and lyophilized to prepare for chromatographic fractionation.

Mutanolysin treatment

A mutanolysin treatment buffer was prepared to a final concentration of 40% sucrose (by weight), 50 mM potassium phosphate dibasic/potassium phosphate monobasic, and 1 mM magnesium dichloride. The bacterial pellets were suspended in the mutanolysin treatment buffer at approximately 0.5 g per mL of buffer and mutanolysin enzyme was added to a concentration of 50 U/mL of enzymatic activity. These

suspensions were then incubated at 37 C overnight while agitated on a shaker rack. During method development gram stains were performed in order to confirm that protoplast formation had been achieved but this was discontinued after the extraction technique was verified.

The mutanolysin treatment suspension was then centrifuged for 30 minutes at 10,000 RCF and 4 C and the aqueous portion of the suspension was harvested, and the pellet was discarded. The resulting aqueous portion was dialyzed using a 3 kDa membrane to remove the high sucrose concentration and any excess salts before being frozen and lyophilized in preparation for chromatographic fractionation.

Fractionation and separation

All the chromatography runs were performed on either a Biorad NGC system or a Biorad [insert model of old FPLC] both systems were equipped with multi-wavelength UV-Vis detectors and refractive index detectors. Where applicable the 206 nm, 260 nm, and 280 nm wavelengths were monitored, and the refractive index detector was equilibrated against the running buffer. The chromatographic systems that were used for the fractionation and separation of biological samples were sterilized and depyrogenated by flushing the system with 5 column volumes of 0.5 M sodium hydroxide followed by 5 column volumes of type I water then equilibrating the system with running buffer.

Size exclusion chromatography

The size exclusion chromatography was performed using either an XK 50/100 or a XK 10/300 column packed with Sephacryl S-300 resin on a Biorad FPLC system. The chromatography system was equilibrated with a 50 mM Tris/Tricene pH 7 buffer with

0.05% sodium azide to prevent bacterial growth. Separation runs were performed at a flow rate of 2 mL per minutes with a total volume of approximately 1.3 column volumes with 3 mL fractions collected throughout the entire run. The runs were separated into 90 fractions which were then pooled into test fractions based on the chromatography data. Fraction size and run times were standardized based on the volume of each specific column.

Samples were prepared by resuspending the lyophilized bacterial extracts in between 10-20 mL of running buffer based on how much material was recovered from the extraction process. These samples were then centrifuged for 5 minutes at 4,000 RCF and 4 C in order to remove any insoluble material. 5 mL of the bacterial extract was loaded on the column, multiple runs were performed and pooled if necessary, and fractionation was determined by chromatographic results. These fractions were then dialyzed using a 3 kDa membrane to remove the running buffer and were then frozen and lyophilized.

Ion exchange chromatography

The ion exchange chromatography was performed using POROS XQ strong anion exchange resin. Separation runs were performed with a running solution of 0.05 M sodium chloride with a stepwise increase of 1 M sodium chloride solution. Sample runs were monitored only using UV-Vis since salt concentrations affect the readings on refractive index detectors.

When working with dried samples they were dissolved in 5 mL of 0.05 M sodium chloride and loaded onto the column. Otherwise, fractions could be loaded onto the Ion exchange column from the size exclusion fractionation so long as the total sample weight

loaded did not exceed the column capacity. Sample runs were fractionated according to a stepwise salt concentration created by increasing the percentage of 1 M sodium chloride present in the eluent mix. Two column volumes of eluent were sufficient to elute material that was responsive to the salt concentration at each gradient. The fractions were then dialyzed using a 3 kDa membrane to remove excess salt from the fraction and were then frozen and lyophilized.

Hydrophobic interaction separations

Samples were separated based on hydrophilicity using a C18 solid phase extraction cartridge. Each C18 cartridge was washed with 5 mL of isopropyl alcohol, followed by 5 mL of methanol, and finally 5 mL of type I water. After washing the cartridge, a known mass of bacterial extract was dissolved in 1 mL of type I water and loaded onto the cartridge. The loading solution was captured along with 4 mL of type 1 water. The column was then eluted with 5 mL of acetonitrile followed by 5 mL of Isopropyl alcohol. The water fraction was frozen and lyophilized while the acetonitrile and isopropyl alcohol fractions were dried down under in a 30 C water bath under ultra purified nitrogen. The mouse experiments performed using these samples were normalized to the initial weight of sample loaded onto the C18 cartridge.

Characterization

NMR spectra analysis

Samples were characterized using a Bruker Avance II 600 MHz NMR system. They were run using a water suppressing proton NMR program and unless otherwise stated were dissolved in deuterium oxide at a concentration of 1 mg per mL.

Gas chromatography Mass Spectroscopy

Carbohydrate analysis of the samples was performed by a collaborator using a standard TMS derivatization modified from Bettigneies-Dutz et al (1997). Sorbitol was added to the sample as an internal standard to compare column performance between runs. Then the sample was loaded onto a GC-MS and compared against a selection of standards.

Enzymatic degradation

For some experiments the degradation of xylose polysaccharides present in the sample was performed. These samples were brought up in 5 mL of 50 mM Tris/Tricene pH 7 buffer and had 100 units of xylanase added to the sample. They were then incubated at 37 C overnight while being agitated. After incubation the samples were centrifuged for 15 minutes at 4,000 RCF and 4 C to pellet any particulate and the supernatant was removed and dialyzed to remove the buffer and degradation products before being frozen and lyophilized.

Tumor model Readout

Mouse types and conditions

Most of the tumor model experiments were performed using 6 week old female germ free mice obtained from the gnotobiotic facility at Harvard medical school. These were selected due to the efficacy noticed in previously done work in these tumor models. This efficacy was measured through both the ability of the tumor cell lines to grow in the mice lineages and the ability for known tumor treatments to have efficacy in the mouse tumor model.

The exceptions to this were the narrow fraction ion exchange experiment where due to sheer number of mice required it was performed in C57BL/6 female mice at 6 weeks old that were purchased from Taconic Biosciences. All mice in the experiments were used following the Kasper lab IACUC protocol and under compliant housing standards.

Tumor types used and dosage schemes

Mice were anesthetized using a 2.5% avertin solution diluted in dubelco's phosphate buffered saline (DPBS). Then under anesthesia they had 2.5×10^5 tumor cells from either the MC38 or B16-OCA tumor lines injected into their abdominal flank. The tumors cells that were used for implantation for each experiment were derived from the same culture mediums and were implanted in all the participating mice on the same day.

The tumor implanted mice began treatment for the experimental conditions and were gavaged with either 100 ug of bacterial extract or an equivalent volume of vehicle starting on day 6 in the initial experiment, and day 7 for all subsequent experiments.

Alongside the gavage of bacterial material an intraperitoneal injection delivered a dose of 100 ug of either an anti-PD-L1 antibody or an equivalent amount of rat IgG2a or rat IgG2b isotype controls.

The tumor size was measured using digital calipers and the volume of the tumors were determined by using the formula for an ellipsoid, $0.5 \times D \times d^2$, where D was the longer diameter of the tumor and d was the shorter. Any mice whose tumors reached 2,000 mm^3 or had become ulcerated were humanely euthanized in accordance with institutional and protocol care conditions.

Chapter III

Results

The primary readout for the efficacy of bacterial fractions is shown through one of the two mouse tumor models that have been previously described. The fractions that are tested were identified and isolated through chromatographic techniques that are shown before the related tumor model experiment.

Size exclusion fractionation

Rough extract from the mutanolysin extraction protocol was used to develop the size exclusion fractionation.

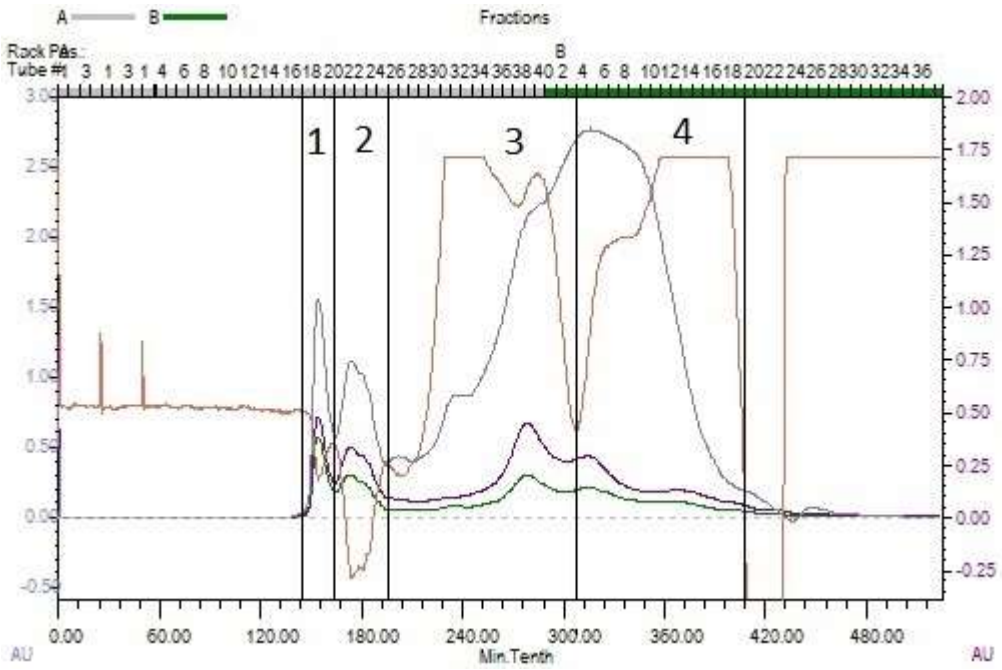

Figure 1. Mutanolysin Extract initial size exclusion chromatography

The orange chromatogram represents the refractive index readout. The blue, purple and green readouts correspond to the 206 nm, 280 nm, and 260 nm absorption. The sample fractions are labeled accordingly.

A tumor model experiment using MC38 cells was run with five sample groups: a control that received 100 ug of anti-PD1 antibodies via intraperitoneal injection and four groups that received the same dose of anti-PD1 as well as 100 ug of the corresponding sample fraction via oral gavage. The treatment was administered on days 6, 9, 12, and 16. Sample fractions were prepared by dissolving lyophilized samples prepared from the size exclusion run at a concentration of 1 microgram per microliter.

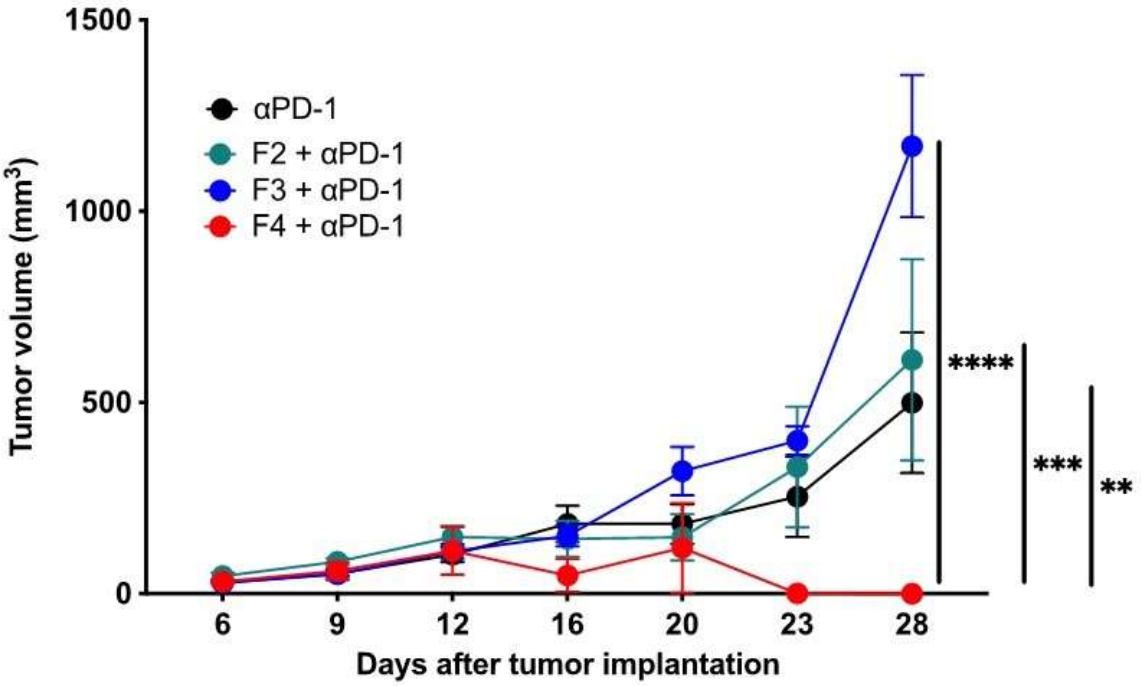

Figure 2. Sample fractions in MC38 tumor model in germ-free mice

Measured tumor volume in mice dosed with sample fractions. The fraction 1 treatment group was removed due to the early euthanasia of most mice in the group due to tumor growth and ulceration. The significances shown were calculated at day 28. It was measured using a two way ANOVA with Turkey's multiple comparisons test, n=5 mice per group the error bars shown display mean and s.e.m.

Broad concentration fractions ion exchange experiment

Material from fraction 4 of the size exclusion chromatography experiment was loaded onto a strong anion exchange column and was eluted in two fractions using a 25% 1 M sodium chloride elution solution followed by a 75% 1 M sodium chloride solution.

A tumor model experiment using MC38 cells was run in antibiotics treated SPF mice acquired from Taconic bioscience. The mice were treated with broad spectrum antibiotics delivered through their water supply beginning seven days before tumor implantation. Three experimental conditions were run, a control using a 100 ug dose of anti-PD-L1 antibodies delivered via intraperitoneal injection on days 7, 10, 13, and 16 and two sample conditions that received the same antibody dose along with 100 ug of the two sample fractions.

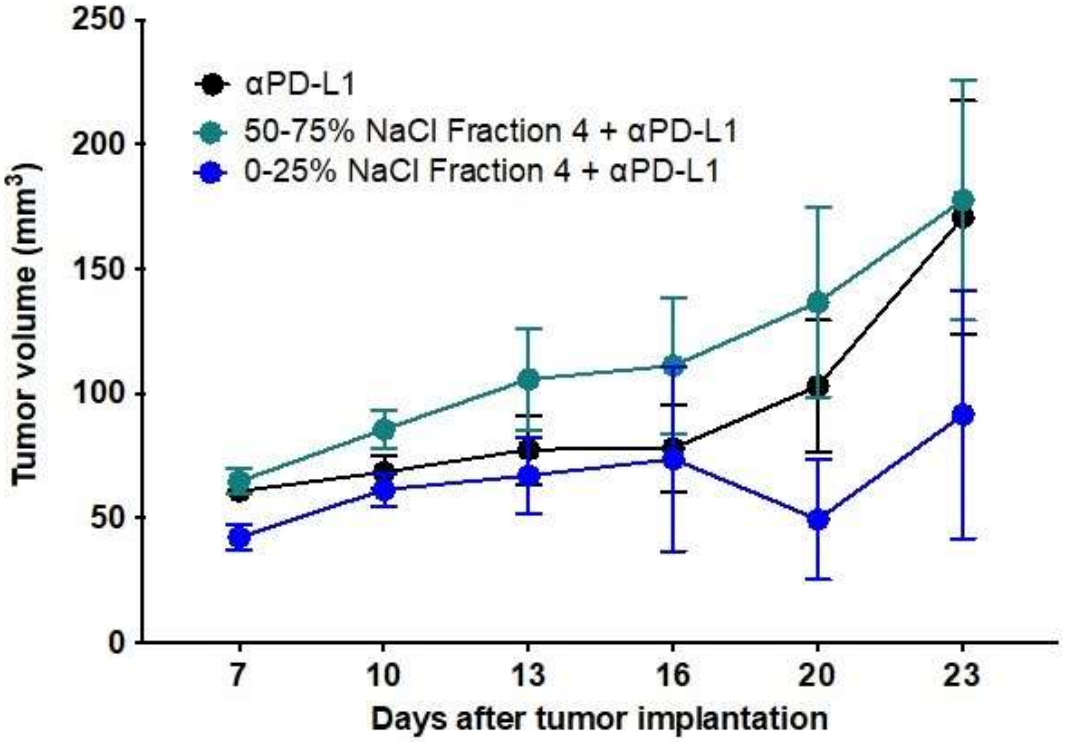

Figure 3. Broad concentration range Ion exchange samples in MC38 tumor model in antibiotics treated SPF mice

The significances shown were calculated at day 23. It was measured using a two way ANOVA with Turkey's multiple comparisons test, n=10 mice per group the error bars shown display mean and s.e.m.

Narrow fraction ion exchange experiment

The initial material for the narrow fraction experiment was taken from the active fraction after the size exclusion separation.

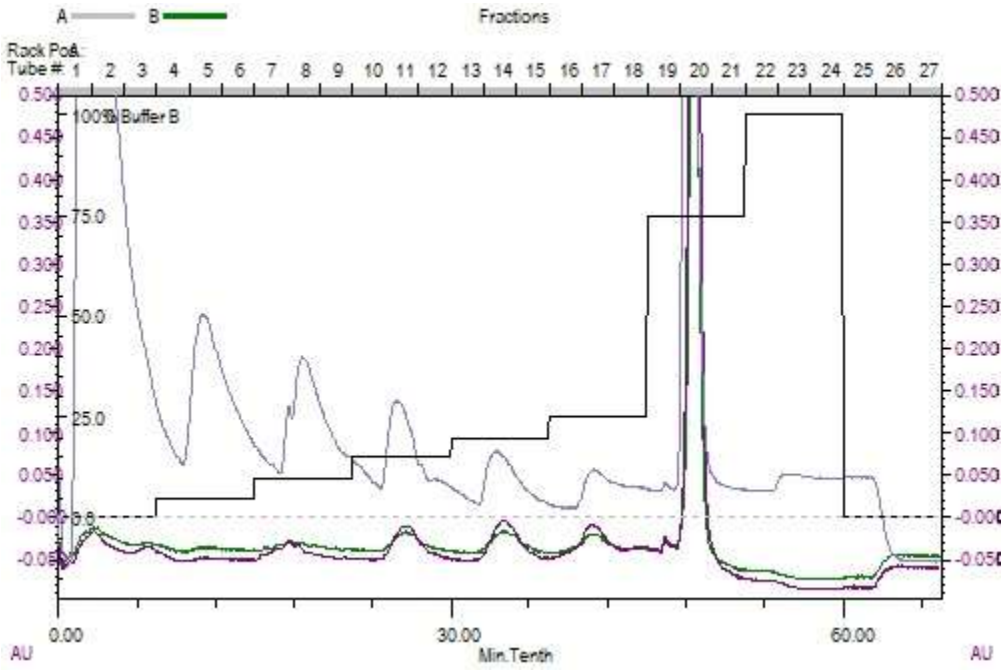

Figure 4. Narrow concentration range Ion exchange run

The active sample fraction from the size exclusion purification step was loaded in 0.05 M sodium chloride onto a POROS XQ strong anion exchange column. Sample fractions were eluted in a stepwise fashion using a 5% increase in the proportion of 1 M sodium chloride eluent up to 25%. The blue, purple and green readouts correspond to the 206 nm, 280 nm, and 260 nm absorption.

A B16-OVA tumor model experiment was run in SPF mice acquired from Taconic Biosciences. Due to the large size of the experiment, it was run in SPF mice. The control group received 100 ug of anti-PD-L1 antibodies via intraperitoneal injection on days 7,

10, 13, and 16. The sample conditions received the same antibody treatment alongside 100 ug of sample via oral gavage.

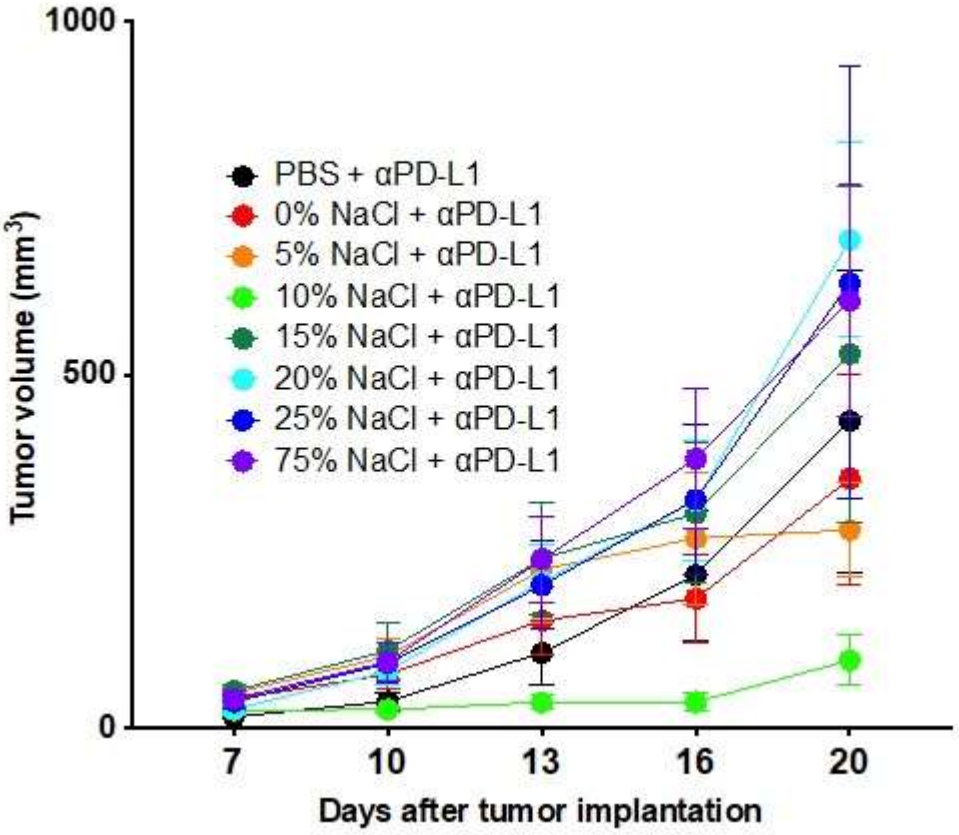

Figure 5. Narrow concentration range Ion exchange samples in B16-OVA tumor model in SPF mice

The significances shown were calculated at day 20. It was measured using a two way ANOVA with Turkey's multiple comparisons test, n=10 mice per group the error bars shown display mean and s.e.m.

10 percent salt concentration experiment

The initial material for the narrow fraction experiment was taken from the active fraction after the size exclusion separation.

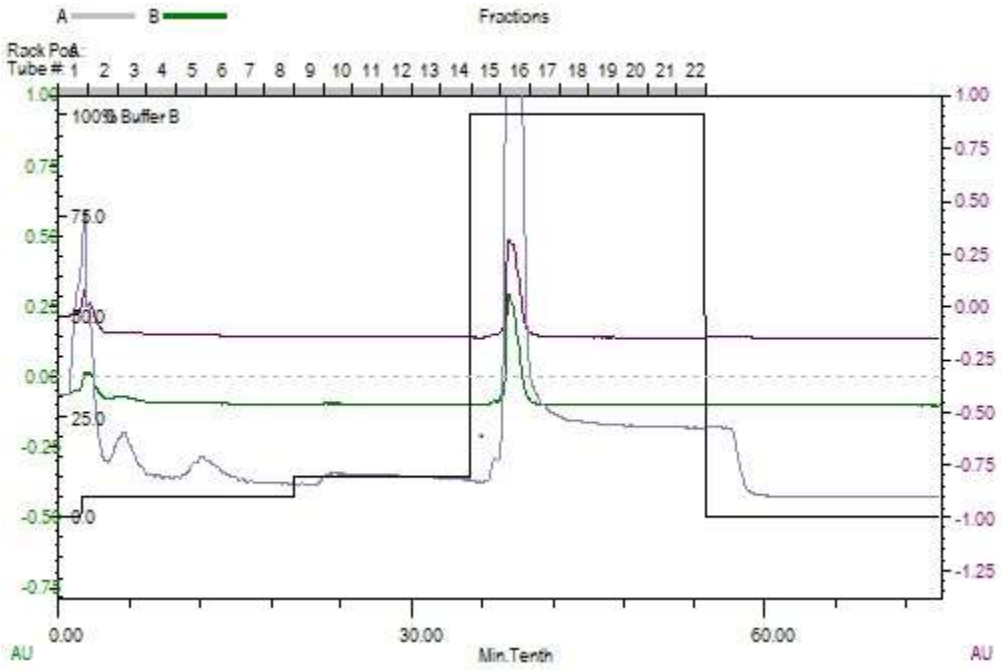

Figure 6. 10 percent fraction isolation

The active sample fraction from the size exclusion purification step was loaded in 0.05 M sodium chloride onto a POROS XQ strong anion exchange column. The column was washed with 5 percent 1 M sodium chloride before eluting the 10 percent fraction. The remaining material was eluted using 100 percent 1 M sodium chloride. The blue, purple and green readouts correspond to the 206 nm, 280 nm, and 260 nm absorption.

An MC38 tumor model experiment was run in germ-free mice. The control group received 100 ug of anti-PD-L1 antibodies via intraperitoneal injection on days 7, 10, 13, and 16. The sample conditions received the same antibody treatment alongside 100 ug of sample via oral gavage.

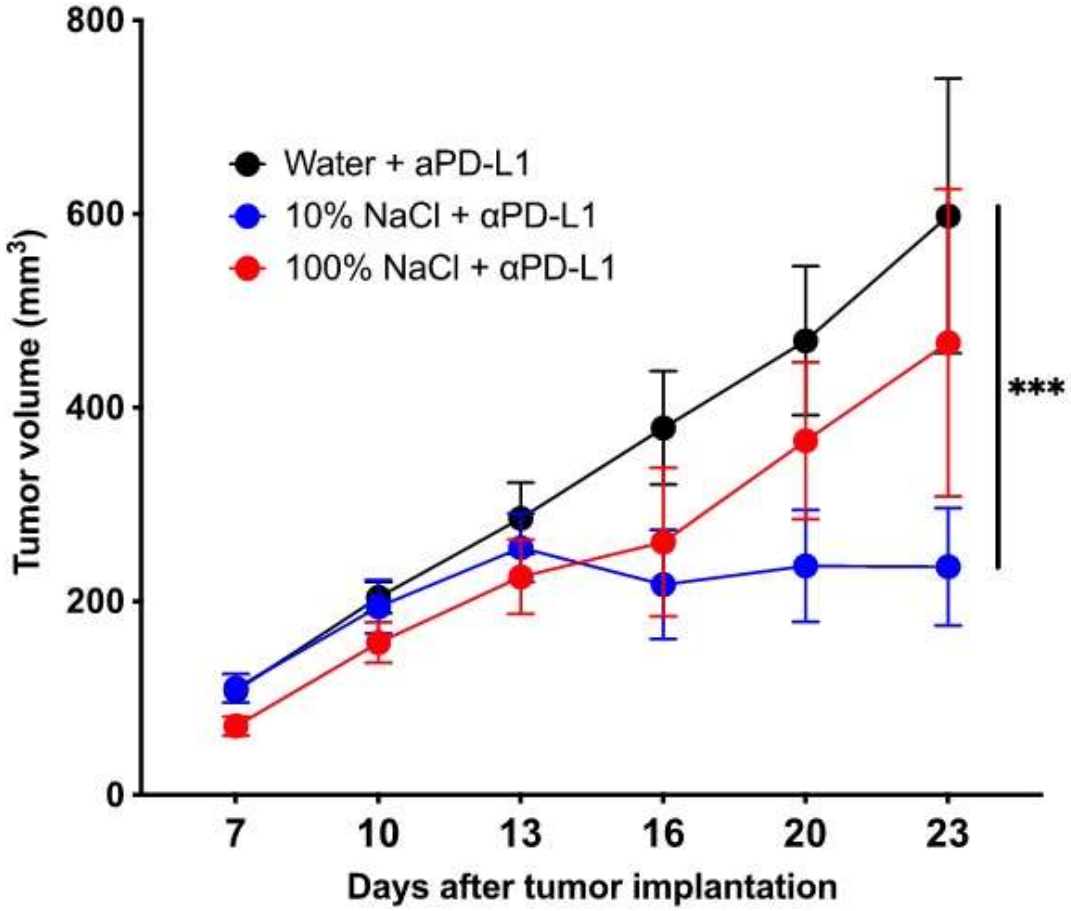

Figure 7. 10 percent salt sample in the MC38 tumor model in germ-free mice

The significances shown were calculated on day 23. It was measured using a two way ANOVA with Turkey's multiple comparisons test, n=10 mice per group the error bars shown display mean and s.e.m.

Extraction technique comparisons

Three 30-liter cultures were grown, and each was subjected to the three proposed extraction methods. The final lyophilized product was weighed and compared before chromatography was performed.

Table 1. Extraction technique results

Extraction technique	Bacterial wet pellet	Rough extract	10 percent salt fraction
Mutanolysin	278 g	4.76 g	33 mg
Bass hydrolysis	320 g	1.43 g	8 mg
Hot Phenol	263 g	1.77	Negligible

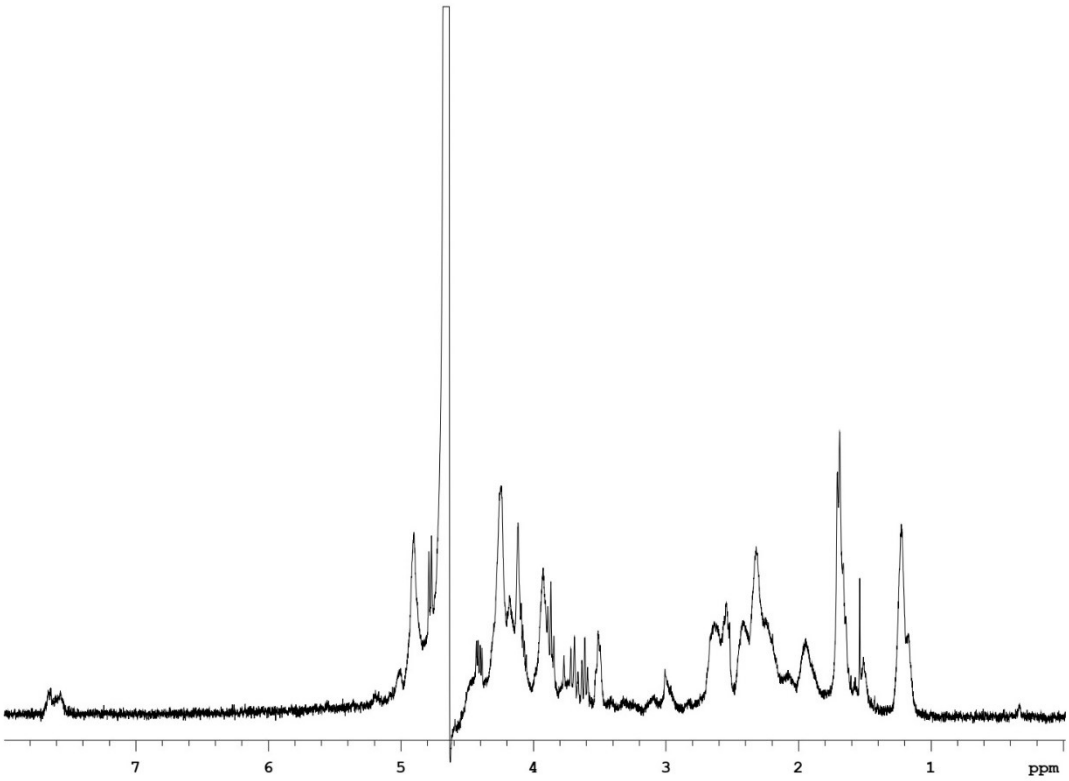

Figure 8. NMR Spectra of mutanolysin extraction 10 percent salt fraction

Proton NMR spectra run on the 10 percent salt fraction of a mutanolysin treated extract. The sample was run at a concentration of 1 mg per mL in deuterium oxide.

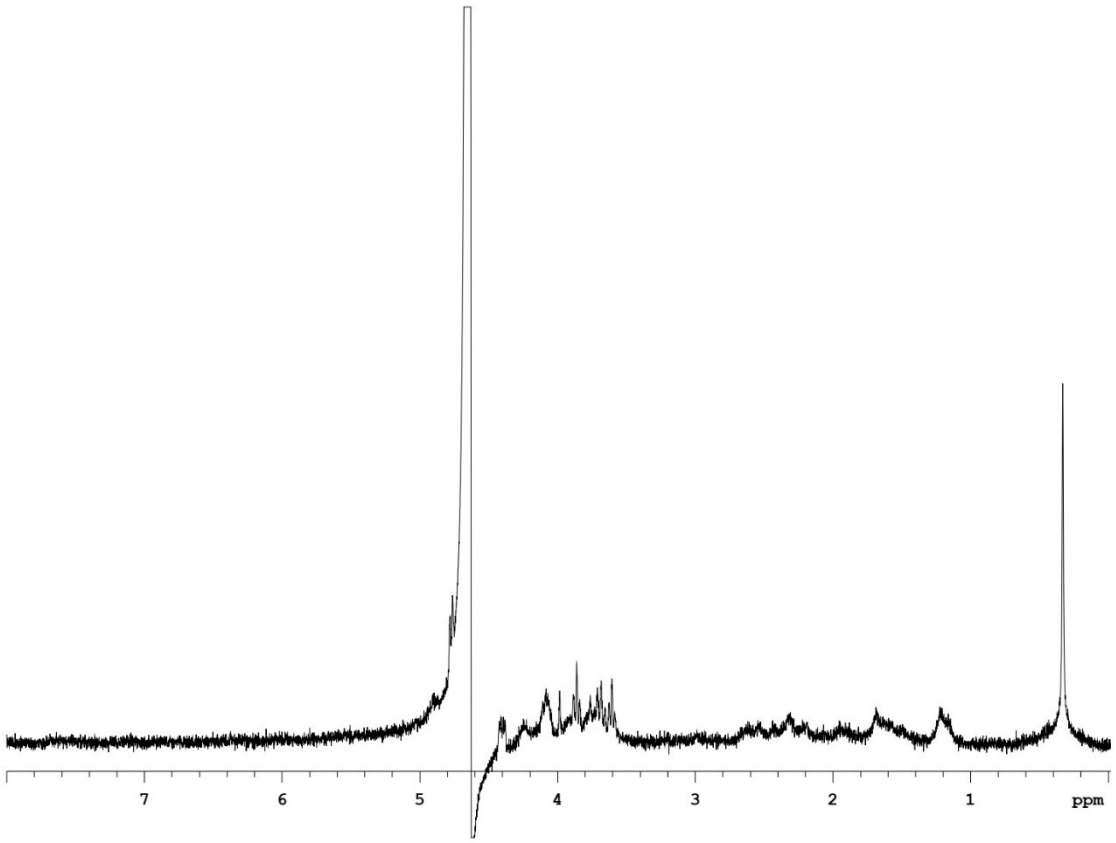

Figure 9. Proton NMR spectra of base hydrolysis extraction 10 percent salt fraction

Proton NMR spectra run on the 10 percent salt fraction of a doc treated extract. The sample was run at a concentration of 1 mg per mL in deuterium oxide.

Enzymatic degradation experiment

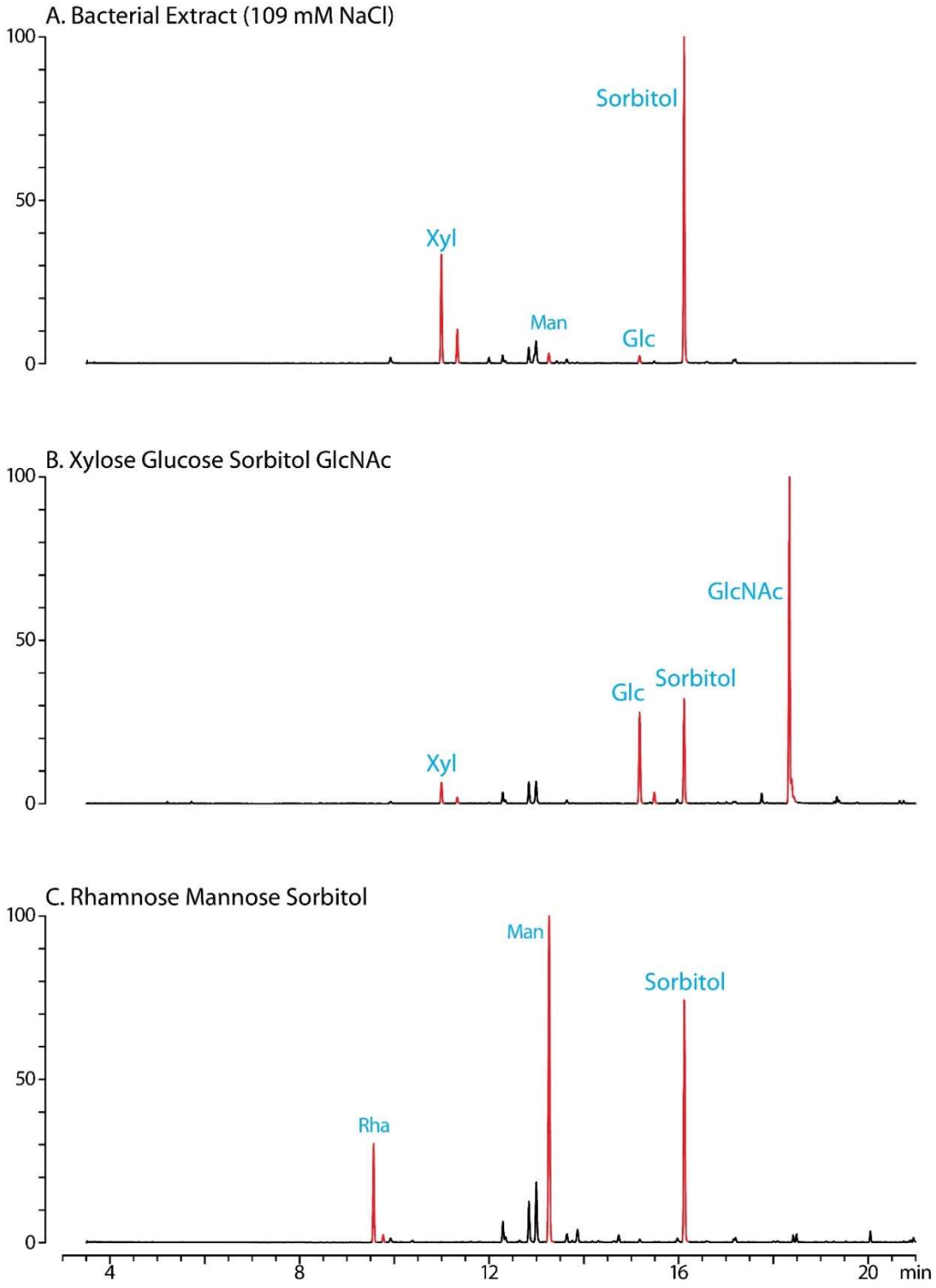

Figure 10. GC-MS analysis carbohydrates in the 10 percent salt fraction

A sample from the 10 percent salt fraction and hexose controls were derivatized using a TMS protocol. The samples were then run on a 15 meter DB–5MS silica column running carrier gas at 1 mL per minute with a Thermo GC-Orbitrap detector. This analysis was performed by Tiandi Yang, a fellow member of the Kasper Lab.

5 mg of the 10 percent salt fraction was treated with xylanase and tested in an MC38 tumor model experiment in germ-free mice. Four experimental conditions were established, an isotype control group that received 100 ug of rat IgG via intraperitoneal injection on days 7, 10, 13, and 16, the three test groups received 100 ug of anti-PD-L1 on the same dosage schedule. The sample conditions received either 100 ug of the 10 percent salt fraction or the equivalent post-xylanase treatment by gavage alongside the antibody treatment.

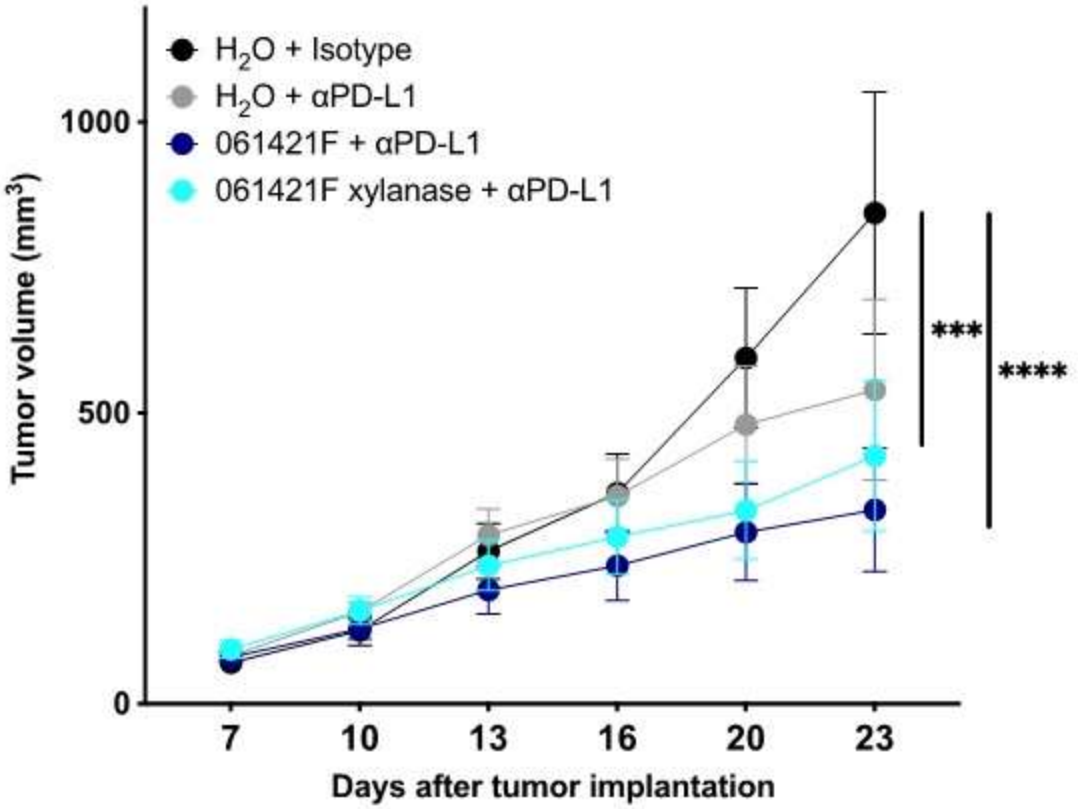

Figure 11. Xylanase treated 10 percent salt fraction in MC38 tumor model in germ-free mice

The significances shown were calculated on day 23. It was measured using a two way ANOVA with Turkey's multiple comparisons test, n=10 mice per group the error bars shown display mean and s.e.m.

Chemical affinity separation experiment

5 mg of 10 percent salt fraction was treated with xylanase and loaded onto a C18 solid phase extraction cartridge. Three sample fractions were recovered and tested in the MC-38 tumor model in germ free mice. The sample dose was nominalized to the starting mass of 10 percent salt fraction that was initially processed and given by oral gavage on days 7, 10, 13, and 16 along with 100 ug of anti-PD-L1 antibody via intraperitoneal injection.

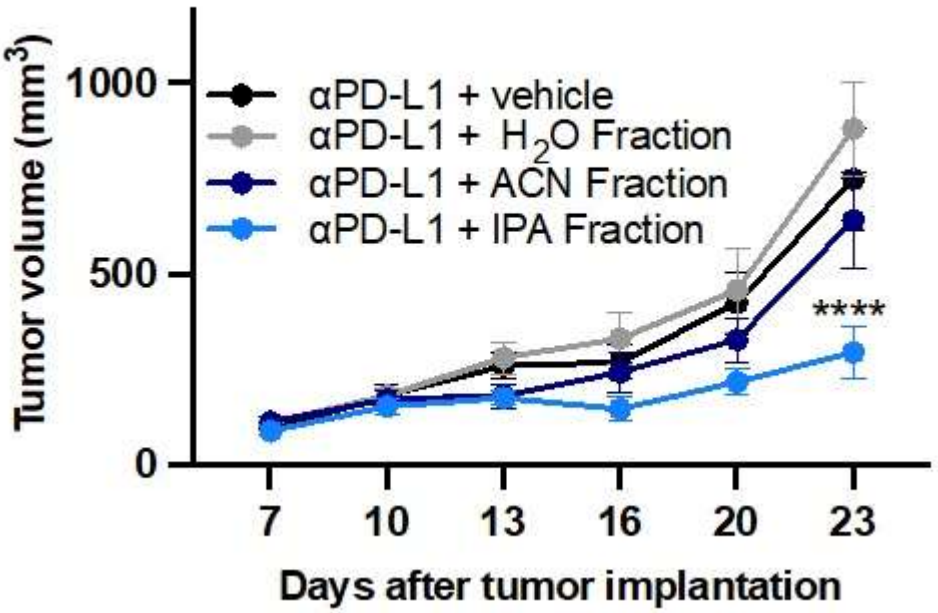

Figure 12. Hydrophobicity separation of the 10 percent salt fraction in the MC38 tumor model in germ-free mice

The significances shown were calculated on day 23. It was measured using a two way ANOVA with Turkey's multiple comparisons test, n=10 mice per group the error bars shown display mean and s.e.m

C18 separation was repeated with 5 mg of 10 percent salt fraction, and the isopropanol fraction was run using an MC38 tumor model in antibiotics treated SPF mice purchased from Taconic biosciences. The sample was dissolved in dimethyl sulfoxide (DMSO) and diluted to a nominal concentration of 1 mg per mL and 10% DMSO. The control group was gavaged with 10% DMSO and given 100 ug of anti-PD-L1 antibody via intraperitoneal injection on days 7, 10, 13, and 16. The sample group was gavaged with a nominal concentration of 100 ug of isopropanol fraction and 100 ug of anti-PD-L1 antibody via intraperitoneal injection on the same schedule.

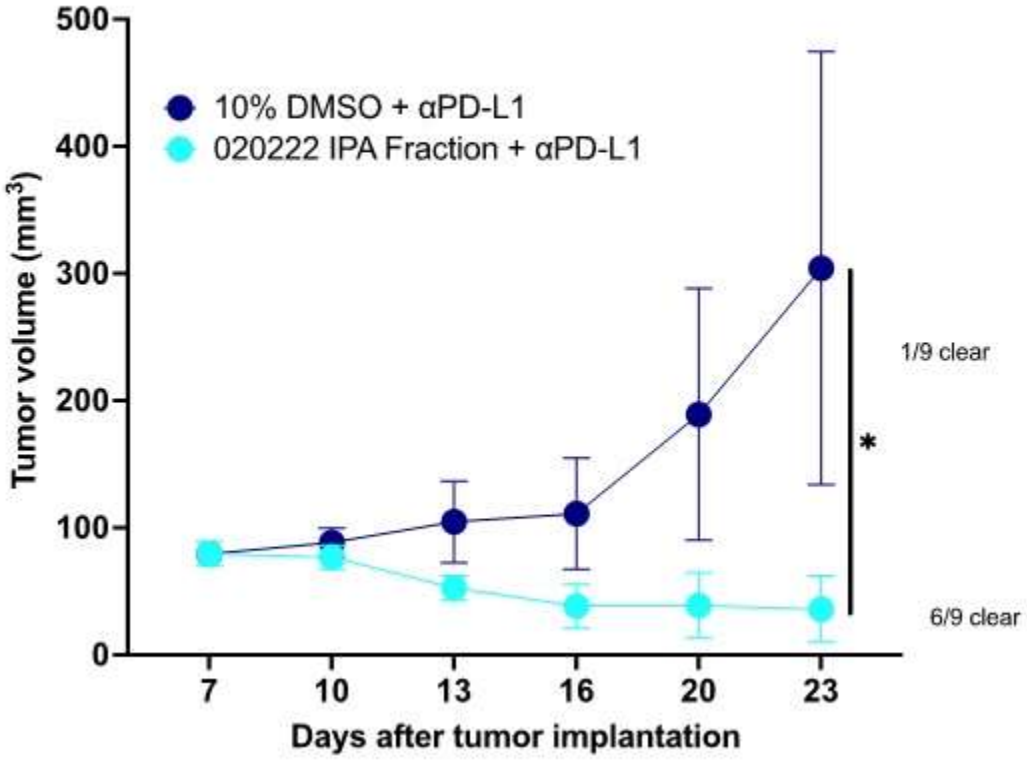

Figure 13. Hydrophobicity separation of the 10 percent salt fraction in the MC38 tumor model in antibiotic treated SPF mice

The significances shown were calculated on day 23. It was measured using a two way ANOVA with Turkey's multiple comparisons test, n=10 mice per group the error bars shown display mean and s.e.m

Chapter IV.

Discussion

C. cateniformis has been shown to improve the outcomes in mouse tumor models. Since this effect was noticed through the oral gavage of dead bacteria, we thought that it was a likely hypothesis that the compounds responsible for the increase in tumor killing efficacy would be some kind of surface associated molecule present as either a primary constituent or simple modification on the bacterial cell wall. We were able to confirm this through the observation of downregulation of PD-L2 in bone marrow dendritic cells (BMDC) (Park 2023). In order to attempt to limit the presence of intracellular bacterial products that would need to be removed from the isolate I set out to modify a mutanolysin based method for bacterial cell wall degradation from Deng et al (2000) to create a rough surface extract that was used in the BMDC assay. The mutanolysin method developed served to remove most of the cell wall from the bacterial extracts while leaving mostly intact spheroplasts.

The column used for the initial size exclusion fractionation was the XK-50/100 packed with S300 HR resin, this was chosen for the efficiency it has with small to medium sized molecules. Since we hypothesized that we were looking for a surface associated carbohydrate the S300 HR resin offered an optimal fractionation range, between two thousand and forty thousand kilodaltons, ensuring that unless the molecule of interest was unusually small or large, we would be able to effectively and efficiently capture it in the chromatographic run.

The initial fractionation chromatography indicated that the samples contained an abundance of carbohydrates and lipids, as indicated by the high intensity of the refractive index. I fractionated the sample run into four fractions: the first fraction contained the flow through portion of the run, all the material that was too large to be captured on the column, the second fraction eluted at the high molecular weight range of the column and due to the proportion of 260nm/280nm it was likely that it contained mostly cell surface proteins, fractions 3 and 4 were separated based on the divide present in the RI signal. The signals in the 206nm, which can be used to detect long chain carbohydrates, showed that there were likely 4 sample peaks that could not be resolved well due to column resolution and sample similarity. Separating the later two fractions at the valley in RI readout created them as a mid-size range and low size range fraction. The results from the mouse tumor experiment clearly showed that the small molecular size fraction, fraction 4, was the most highly enriched with immunogenic molecules and was established as the sample of interest. Since there was very little signal shown after fraction 4 I determined that there were likely very few small molecular components that were present in the sample and due to constraints on the animal model did not create a fraction that would represent them. Had I not been able to identify a fraction from the four that were created that possessed the improved tumor killing that the unfractionated sample had shown the small molecules in the flow through would have been the obvious next site of inquiry.

The high response in both the RI and 206 nm signals gave a strong indication that the immunogenic molecule I was interested in was part of a molecular structure that contained a polysaccharide component. This was partially differentiated from the possibility of it being a large lipid compound since I was able to isolate it on the smaller

side of the size exclusion run while it was performed in a neutral aqueous running buffer. If the molecule of interest was simply a medium to large sized lipid it would likely form micelles that would be of sufficient globular size to elute from the size exclusion column in fraction 1.

Since polysaccharides often contain charged chemical moieties, I decided to perform a second purification step using a strong anion exchange column. It is common in bacterial polysaccharides to have a high number of oligosaccharide repeating units that can contain charged sugars, so I chose to perform a broad separation over a large salt concentration gradient. I chose to load the column with the material in 0.05 M sodium chloride solution and eluting fractions with 25 % 1 M sodium chloride and 75% 1M sodium chloride. The 100% 1 M sodium chloride wash of the column was not tested due to limitations with the number of mice available for the tumor mouse model at the time. The results from the tumor experiment did not reveal a statistically significant difference between the two experimental conditions at the end of day 23. This was in part thought to be due to there not being significant tumor growth in any of the conditions that were performed. However, while the tumor volume did not indicate a significant difference the presence of mice that had completely cleared the tumor in the 25% sodium chloride fraction indicated that further fractionation in the lower salt concentration gradient was a useful next step.

I then repeated the salt fractionation using a narrow concentration gradient, increasing the eluent by five percent in each step. I believed if the immunomodulatory molecule was being captured at low salt concentrations this was the most likely experimental setup to garner an effective fraction and have sufficient sample for the

experiment. The chromatogram indicates that most of the material that was loaded on to the column eluted with the loading solvent (0.05 M sodium chloride) and the final column wash (1 M sodium chloride). The results from the mouse tumor experiment showed strong indications that the 10 percent salt fraction contained the highest concentration of immunomodulatory molecules.

In order to finally confirm that the 10 percent fraction was the only significantly effective fraction in the mouse tumor model I isolated the 10 percent fraction and the 100 percent salt fraction and compared them in the mouse tumor model. This experiment confirmed that the 10 percent salt fraction was effective in the tumor model. I had now established an instrumental purification technique that produced a bacterial fraction that was immunogenically active and significantly increased the efficacy of tumor killing however the raw material that this process yielded was low and presented an obstacle to further analysis and purification, because of this I pursued other forms of chemical purification in hope of a higher final yield.

We grew two batches of *C. cateniformis* and I performed the two chemical extraction processes, a hot phenol extraction and the base hydrolysis, that have been used in our lab for the isolation of immunomodulatory molecules from bacteria in the past. The rough extracts that were obtained from the chemical extraction techniques were processed using the same instrumental conditions for the size exclusion and ion exchange steps as the material purified from the mutanolysin bacterial extract. These two extraction processes were chosen specifically because they were effective in isolating bacterial compounds whose main constituents were polysaccharides. The hot phenol extraction did not yield an appreciable amount of material after the column purification steps and the

base hydrolysis method yielded an even smaller amount of material than the mutanolysin extract. This was true of both methods even at the rough extract stage. I had originally thought that the lower yields at the rough extract stage were due to the more specific nature of the chemical extractions versus the mutanolysin extract but the significantly lower yields at the end of the column purification indicated that even if they were isolating the same immunogenic molecules the decrease in yield made them less effective methods.

I compared the material obtained from the base hydrolysis extraction method to the mutanolysin fraction using NMR spectroscopy and identified that the material isolated did not appear to be comparable to the sample of mutanolysin extracted material. The combination of the mismatched NMR profile and the lower yield of the extraction technique led me to decide not to pursue the base hydrolysis as a possible extraction method. It is likely that neither of these extraction processes were effective because both alternative extraction procedures include steps that create harsh chemical environments. These environments may have caused the degradation of the immunomodulatory molecule or might have altered the chemical moieties in a way that significantly modified its behavior on either the size exclusion or strong ion exchange columns. These factors led to the abandonment of alternative chemical extraction techniques since they would require completely reworking the column purification process and were not guaranteed to yield material that was chemically similar to the mutanolysin extraction.

With an effective immunomodulatory fraction isolated through the mutanolysin extraction technique and subsequent size exclusion and ion exchange purifications I began the characterization process. The first step was to perform an analysis of sugars

present in the sample to get a better idea about the polysaccharide structure. The sugar analysis, performed by Tiandi Yang, showed that the primary sugar present in the bacterial extract was xylose. To determine if this was due to a significant presence of xylan, a xylose polysaccharide, we used a commercially available xylanase enzyme to degrade the 10 percent salt fraction. This would ensure that any xylan polysaccharide structures would be degraded into smaller pieces, either single sugars or small oligosaccharides, that we would be able to remove from the sample using filtration techniques.

After processing 5 mg of the 10 percent salt fraction with xylanase the mass of the sample was reduced to approximately 0.5 mg. The xylanase treated sample was tested in the MC38 mouse tumor model using germ free mice. The test showed that the xylanase treated sample along with the original sample prior to treatment were both effective in enhancing tumor killing. This was evidence that the immunomodulatory effect was not reliant on the presence of a xylanase digestible polysaccharide. The lack of reliance however did not eliminate the possibility that the immunogenic molecule was linked to a xylan polysaccharide on the cell surface. Since I knew that the effect did not rely on the polysaccharide component of the sample,

I was able to turn to trying to isolate the only other two categories of biological molecules that could be responsible for the effect, cell surface associated proteins and lipids.

The next step in characterization was separating the sample further in order attempt to identify the chemical characteristics of the immunomodulatory molecule. By using a C18 SPE cartridge I was able to separate the sample based on the hydrophobicity

of the sample. I xylanase digested 5 mg of the 10 percent salt fraction and loaded it onto the SPE cartridge, by using acetonitrile and isopropyl alcohol I was able to create three fractions that would isolate the biological categories of interest. Molecules without any hydrophobic moieties would elute through the column while the sample was loaded, mildly hydrophobic molecules, such as many surface associated proteins, would elute using acetonitrile, and hydrophobic molecules, such as lipids, would elute with isopropyl alcohol. Since I knew that the compound was soluble in water it was likely that if the compound was a lipid, it would be hydrophilic enough to not need an organic solvent, such as hexane, to elute from the cartridge avoiding the complication of extracting any contaminants from the plastic of the cartridge.

The samples were run in the mouse tumor model using the nominal concentration that was loaded onto the C18 SPE before elution. An equivalent of 100 ug of each elution condition was dosed via gavage alongside the anti-PD-L1 antibodies in both germ-free mice. The SPE separation was repeated without xylanase treatment and the isopropanol fractions enhancement of tumor killing was confirmed in an experiment using antibiotics treated mice from Taconic Biosciences. In both experiments the isopropanol fraction was shown to significantly enhance the tumor killing effects of an anti-PD-L1 antibody treatment regime.

The results of these separations and experiments indicate the isolation of an immunomodulatory fraction from the mutanolysin treated *C. cateniformis* bacterial pellet between the approximate sizes of 2-20 kDa with significant but low binding affinity on a strong anionic ion exchange column confirming that it was a surface bound molecule that was responsible for the enhancement of tumor killing in the mouse tumor models. The

molecule of interest may be bound to a xylan polysaccharide, but the presence of the polysaccharide is not necessary for the enhancement of tumor killing in the mouse model. The results of the C18 SPE experiments indicate that the immunomodulatory molecule has a strong hydrophobic moiety, indicating that it is likely to contain a lipid, and if it is bound to the xylan polysaccharide the hydrophobic moiety causes it to elute with isopropyl alcohol in that circumstance. The hydrophobicity of the compound as well as the intensity of the low ppm signals in the NMR signal after C18 separation are strong suggestions that the immunomodulatory molecule is a bacterial lipid.

Knowing that the immunomodulatory molecule is likely to be a bacterial lipid, the identification of the exact type and structure of the immunomodulatory molecule is the obvious next step. This presents a significant technical challenge as it is possible that there is a mix of lipids present in the final active fraction. Separating lipids of similar molecular size is going to require the application of more advanced high pressure liquid chromatographic techniques. These techniques have the advantage of accurate and reproducible separation of lipid species based on small modifications in their chemical structure. This strength is also one of the techniques weaknesses, in addition to the inherent sample loss that occurs whenever a column run is performed it is likely that this will require a high number of fractions being generated if there is a wide variety of lipids present. If this HPLC technique is necessary, then in order to produce bacterial material in sufficient quantity to perform *in vivo* experiments it will likely necessitate completely reworking the extraction and purification procedures to focus on surface lipid extraction.

This highlights one of the current limits of the work, our only confirmed way of testing the efficacy of our samples is the use of a month-long mouse model that requires a

significant amount of sample material. We are currently working to develop an *in vitro* model that we can trust has the same predictive power as the mouse model. This would significantly decrease the amount of material required to test sample fractions and allow for more powerful analytical scale techniques to be used.

The isolation of a suspected surface associated lipid from *C. cateniformis* is in line with other research that has shown small bacterial metabolites and structural components can have important immunomodulatory effects in the tumor model. Furthermore, it is evidence of the importance of this kind of interdisciplinary approach to identifying the causes of immunological activity in disease models. Through working to identify the immunological mechanism and the molecule responsible for its activation we can develop novel therapeutics that may serve to improve the tolerance and efficacy of current treatment modalities.

References

Agilent. (2016). *The LC Handbook: Guide to LC Columns and Method Development*. https://www.agilent.com/cs/library/primers/Public/LC-Handbook-Complete-2.pdf

American Cancer Society. (2023). *Cancer facts and figures* https://www.cancer.org/research/cancer-facts-statistics/all-cancer-facts-figures/2023-cancer-facts-figures.html

Baruch, E. N., Youngster, I., Ben-Betzalel, G., Ortenberg, R., Lahat, A., Katz, L., ... & Boursi, B. (2021). Fecal microbiota transplant promotes response in immunotherapy-refractory melanoma patients. *Science*, 371(6529), 602-609.

De Bettignies-Dutz, A., Reznicek, G., Kopp, B., & Jurenitsch, J. (1991). Gas chromatographic—mass spectrometric separation and characterization of methyl trimethylsilyl monosaccharides obtained from naturally occurring glycosides and carbohydrates. *Journal of Chromatography A*, 547, 299-306.

Chung, H., Pamp, S. J., Hill, J. A., Surana, N. K., Edelman, S. M., Troy, E. B., ... & Kasper, D. L. (2012). Gut immune maturation depends on colonization with a host-specific microbiota. *Cell*, 149(7), 1578-1593.

Coussens, L. M., & Werb, Z. (2002). Inflammation and cancer. *Nature*, 420(6917), 860-867.

Cytiva. (2020). *Size Exclusion Chromatography: Principles and methods.* https://cdn.cytivalifesciences.com/api/public/content/digi-11639-pdf

Cytiva. (2021). *Ion Exchange Chromatography: Principles and methods*. https://cdn.cytivalifesciences.com/api/public/content/digi-13101-pdfcyt

Davar, D., Dzutsev, A. K., McCulloch, J. A., Rodrigues, R. R., Chauvin, J. M., Morrison, R. M., ... & Zarour, H. M. (2021). Fecal microbiota transplant overcomes resistance to anti–PD-1 therapy in melanoma patients. *Science*, 371(6529), 595-602.

Deng, L., Kasper, D. L., Krick, T. P., & Wessels, M. R. (2000). Characterization of the linkage between the Type III capsular polysaccharide and the bacterial cell wall of group B Streptococcus. *Journal of Biological Chemistry*, 275(11), 7497-7504.

Erturk-Hasdemir, D., Oh, S. F., Okan, N. A., Stefanetti, G., Gazzaniga, F. S., Seeberger, P. H., ... & Kasper, D. L. (2019). Symbionts exploit complex signaling to educate

the immune system. *Proceedings of the National Academy of Sciences*, 116(52), 26157-26166.

Gopalakrishnan, V., Spencer, C. N., Nezi, L., Reuben, A., Andrews, M. C., Karpinets, T., ... & Wargo, J. (2018). Gut microbiome modulates response to anti–PD-1 immunotherapy in melanoma patients. *Science*, 359(6371), 97-103.

Griffin, M. E., Espinosa, J., Becker, J. L., Luo, J. D., Carroll, T. S., Jha, J. K., ... & Hang, H. C. (2021). Enterococcus peptidoglycan remodeling promotes checkpoint inhibitor cancer immunotherapy. *Science*, 373(6558), 1040-1046.

Han, Y., Liu, D., & Li, L. (2020). PD-1/PD-L1 pathway: current researches in cancer. *American journal of cancer research*, 10(3), 727.

Haslam, A., & Prasad, V. (2019). Estimation of the percentage of US patients with cancer who are eligible for and respond to checkpoint inhibitor immunotherapy drugs. *JAMA network open*, 2(5), e192535-e192535.

Jacobs, J. F., Nierkens, S., Figdor, C. G., de Vries, I. J. M., & Adema, G. J. (2012). Regulatory T cells in melanoma: the final hurdle towards effective immunotherapy?. *The lancet oncology*, 13(1), e32-e42.

Juneja, V. R., McGuire, K. A., Manguso, R. T., LaFleur, M. W., Collins, N., Haining, W. N., ... & Sharpe, A. H. (2017). PD-L1 on tumor cells is sufficient for immune evasion in immunogenic tumors and inhibits CD8 T cell cytotoxicity. *Journal of Experimental Medicine*, 214(4), 895-904.

Kouidhi, S., Ben Ayed, F., & Benammar Elgaaied, A. (2018). Targeting tumor metabolism: a new challenge to improve immunotherapy. *Frontiers in immunology*, 9, 353.

LaFleur, M. W., Muroyama, Y., Drake, C. G., & Sharpe, A. H. (2018). Inhibitors of the PD-1 pathway in tumor therapy. *The Journal of Immun*ology, 200(2), 375-383.

Leach, D. R., Krummel, M. F., & Allison, J. P. (1996). Enhancement of antitumor immunity by CTLA-4 blockade. Science, 271(5256), 1734-1736.

Marabondo, S., & Kaufman, H. L. (2017). High-dose interleukin-2 (IL-2) for the treatment of melanoma: safety considerations and future directions. *Expert Opinion on Drug Safety*, 16(12), 1347-1357.

Marion, D. (2013). An introduction to biological NMR spectroscopy. *Molecular & Cellular Proteomics*, 12(11), 3006-3025.

Matson, V., Fessler, J., Bao, R., Chongsuwat, T., Zha, Y., Alegre, M. L., ... & Gajewski, T. F. (2018). The commensal microbiome is associated with anti–PD-1 efficacy in metastatic melanoma patients. *Science*, 359(6371), 104-108.

Park, J. S., Gazzaniga, F. S., Wu, M., Luthens, A. K., Gillis, J., Zheng, W., ... & Sharpe, A. H. (2023). Targeting PD-L2–RGMb overcomes microbiome-related immunotherapy resistance. *Nature*, 1-9.

Pasche, B. (2001). Role of transforming growth factor beta in cancer. *Journal of cellular physiology*, 186(2), 153-168.

Ribas, A., & Wolchok, J. D. (2018). Cancer immunotherapy using checkpoint blockade. *Science*, 359(6382), 1350-1355.

Seliger, B., Maeurer, M. J., & Ferrone, S. (1997). TAP off—tumors on. *Immunology today,* 18(6), 292-299.

Sivan, A., Corrales, L., Hubert, N., Williams, J. B., Aquino-Michaels, K., Earley, Z. M., ... & Gajewski, T. F. (2015). Commensal Bifidobacterium promotes antitumor immunity and facilitates anti–PD-L1 efficacy. *Science*, 350(6264), 1084-1089.

Snyder, A., Makarov, V., Merghoub, T., Yuan, J., Zaretsky, J. M., Desrichard, A., ... & Chan, T. A. (2014). Genetic basis for clinical response to CTLA-4 blockade in melanoma. *New England Journal of Medicine*, 371(23), 2189-2199.

Tan, S., Li, D., & Zhu, X. (2020). Cancer immunotherapy: Pros, cons and beyond. *Biomedicine & Pharmacotherapy*, 124, 109821.

Tanoue, T., Morita, S., Plichta, D. R., Skelly, A. N., Suda, W., Sugiura, Y., ... & Honda, K. (2019). A defined commensal consortium elicits CD8 T cells and anti-cancer immunity. *Nature*, 565(7741), 600-605.

Van Allen, E. M., Miao, D., Schilling, B., Shukla, S. A., Blank, C., Zimmer, L., ... & Garraway, L. A. (2015). Genomic correlates of response to CTLA-4 blockade in metastatic melanoma. *Science*, 350(6257), 207-211.

Vétizou, M., Pitt, J. M., Daillère, R., Lepage, P., Waldschmitt, N., Flament, C., ... & Zitvogel, L. (2015). Anticancer immunotherapy by CTLA-4 blockade relies on the gut microbiota. *Science*, 350(6264), 1079-1084.

Zamarron, B. F., & Chen, W. (2011). Dual roles of immune cells and their factors in cancer development and progression. *International journal of biological sciences*, 7(5), 651.

Zhao, B., Zhao, H., & Zhao, J. (2020). Efficacy of PD-1/PD-L1 blockade monotherapy in clinical trials. *Therapeutic advances in medical oncology*, 12, 1758835920937612.

Zou, W. (2006). Regulatory T cells, tumour immunity and immunotherapy. *Nature Reviews Immunology*, 6(4), 295-307.

Wu, C. (2004). *Handbook of size exclusion chromatography and related techniques*. Marcel Dekker.